I&EC research
Industrial & Engineering Chemistry Research

Article

pubs.acs.org/IECR

Modification of Hydroxyapatite with Ion-Selective Complexants: 1-Hydroxyethane-1,1-diphosphonic Acid

Yasmine Daniels,[†,‡] Nathalie Lyczko,[§] Ange Nzihou,[§] and Spiro D. Alexandratos*[,†,‡]

[†]Department of Chemistry, Graduate Center of the City University of New York, 365 Fifth Avenue, New York, New York 10016, United States

[‡]Department of Chemistry, Hunter College of the City University of New York, 695 Park Avenue, New York, New York 10065, United States

[§]Université de Toulouse, Ecole des Mines d'Albi, CNRS, Centre RAPSODEE, Campus Jarlard, F-81013 Albi cedex 09, France

Supporting Information

ABSTRACT: Hydroxyapatite (HAP) was modified with 1-hydroxyethane-1,1-diphosphonic acid (HEDP), and its effect on divalent metal ion binding was determined. HAP was synthesized from calcium hydroxide and phosphoric acid. After calcination, it was modified with HEDP, and the influence of time and temperature on the modification was investigated. HEDP incorporation increased as its initial solution concentration increased from 0.01 to 0.50 M. Unmodified and modified HAP were characterized using Fourier transform infrared spectroscopy, X-ray diffraction, scanning electron microscopy, energy dispersive X-ray spectroscopy, and specific surface area analysis. Ca/P ratios, acid capacities, and phosphorus elemental analyses gave the effect of modification on composition and surface characteristics. A high reaction temperature produced new phosphonate bands at 993, 1082, and 1144 cm^{-1} that indicated the presence of HEDP. HAP modification at a high temperature−long reaction time had the highest HEDP loading and gave the sharpest XRD peaks. The emergence of new HAP−HEDP strands was observed in SEM images for treated samples while EDS showed high phosphorus contents in these strands. Modified HAP had a high acid capacity from the additional P−OH groups in HEDP. The P(O)OH groups maintain their ability to bind metal ions within the HAP matrix: contacting the modified HAP with 10^{-4} N nitrate solutions of five transition metal ions gives an affinity sequence of Pb(II) > Cd(II) > Zn(II) > Ni(II) > Cu(II). This result is comparable to that of commercially available di(2-ethylhexyl)phosphoric acid, a common solvent extractant, and the trend is consistent with the Misono softness parameter of metal ion polarizabilities.

INTRODUCTION

Hydroxyapatite (HAP) has a chemical composition similar to bones and teeth.[1,2] Methods to prepare it include reacting calcium nitrate with phosphoric acid,[3] disodium creatine phosphate,[4] ammonium hydrogen phosphate,[5] and phosphorus pentoxide,[6] as well as combining calcium hydroxide with phosphoric acid.[7] Temperature and pH may be adjusted to control physical properties, including mechanical strength, particle size, and pore size.[8−11] During synthesis and drying, the calcium phosphate goes through intermediate amorphous stages until the thermodynamically stable phase is formed with a Ca/P ratio of 1.67.[12−14] The Ca/P ratio can vary between 1.5−1.67 and is affected by reaction time and reactant concentration.[15−17] Drying temperature and duration influence the final structure and degree of crystallinity. Methods for drying HAP include autoclaving,[18] freeze-drying,[19] and thermal treatment.[20,21]

The increasing effect of water pollution on disease has created a need to remove toxic metal ions, including copper, chromium, lead, mercury, and arsenic.[22] HAP has been modified to produce hybrids,[23] microtubes,[24] and ordered arrays[25] and may have an important role in environmental remediation due to its ability to sequester metal ions.[26,27] It is less expensive than ion exchange resins and can be valorized by combining with cement to build infrastructure after sorbing the ions.[28,29] It is stable at neutral pH and can be applied to groundwater treatment.[30] HAP can sorb these ions by ion exchange,[31−33] surface complexation,[34,35] and dissolution/precipitation.[36] It has been immobilized in organic polymers to increase their sorption capacities.[37] The affinity for Pb^{2+} increased when increasing amounts of HAP were incorporated into a polyacrylamide hydrogel[38] and when coated onto polyurethane foam.[39]

This report focuses on HAP and its modification with 1-hydroxyethane-1,1-diphosphonic acid (HEDP) in order to enhance its affinity for metal ions from aqueous solutions. HAP is prepared from $Ca(OH)_2$ rather than calcium nitrate and H_3PO_4 thus obviating the need to wash the product free of nitrate ions.[40] HEDP is one of a group of bisphosphonates that adsorb onto HAP at near-ambient temperatures[41−43] and has a good affinity for metal ions.[44,45] To identify the conditions that give the most HEDP incorporation (rather than only surface modification), calcined HAP was suspended in 0.01−0.50 M HEDP at moderate (20 °C) and high (80 °C) temperatures for short (4 h), long (168 h), and very long (720 h) times. Since $Ca(OH)_2$ is produced from lime, an inexpensive starting material, determining how HAP can be modified to have

Received: October 22, 2014
Revised: December 28, 2014
Accepted: December 29, 2014
Published: December 29, 2014

DOI: 10.1021/ie504181z
Ind. Eng. Chem. Res. 2015, 54, 585−596

significant selectivity for transition metal ions will provide a low-cost alternative to polystyrene-based ion exchange resins.

EXPERIMENTAL SECTION

Synthesis of HAP. HAP was synthesized from calcium hydroxide and phosphoric acid at an initial Ca:P molar ratio of 1.78.[46] In a typical experiment, 3.86 g of $Ca(OH)_2$ was combined with 140 mL of H_2O and 2 mL of H_3PO_4, then stirred for 48 h while maintaining a pH of 8.0−8.2 with dilute H_3PO_4 or KOH solutions. The particles obtained by precipitation were isolated by filtration, dried at ambient conditions and then in a vacuum oven at 60 °C, and calcined at 700 °C for 3 h to obtain HAP with a Ca/P molar ratio of 1.52. This differs from the structure with the stoichiometric value of 1.67 in having a greater quantity of free phosphorus acid sites. As noted below, the significance of this difference was studied.

SYNTHESIS OF mHAP

Calcined HAP was modified by suspending it in 0.01−0.50 M HEDP with pH adjusted to 7.6 to prevent dissolution of the HAP. In a typical experiment, 2.0 g of HAP was added to 100 mL of an HEDP solution, and the reaction was stirred at 20° or 80 °C for 4, 168, or 720 h. The conditions for the different mHAPs are given in Table 1. The final suspensions were filtered, washed with deionized water, and dried at ambient temperature for 48 h.

Table 1. Conditions for the Synthesis of mHAP

	HEDP concn ($mol \cdot L^{-1}$)	reaction temp (°C)	reaction time (h)
mHAP1	0.01	80	168
mHAP2	0.05	80	168
mHAP3	0.10	80	168
mHAP4	0.20	80	168
mHAP5A	0.50	80	168
mHAP5B	0.50	80	4
mHAP5C	0.50	80	720
mHAP6A	0.50	20	168
mHAP6B	0.50	20	4
mHAP6C	0.50	20	720
sHAP1	0		
sHAP2	0.50	80	168
cHAP	0	80	168
Ca−HEDP	0.50	80	168

Control experiments of HAP in water at the same modification times and temperatures were done. Results for the sample prepared at 168 h and 80 °C (cHAP) are reported. Stoichiometric HAP (sHAP1) with a Ca/P ratio of 1.67 was purchased from Sigma-Aldrich and modified with HEDP for 168 h at 80 °C (sHAP2) in order to determine whether the ratio had an effect on the modification.

Synthesis of Ca−HEDP. The calcium salt of HEDP was prepared by adding 1.47 g of $Ca(OH)_2$ to 100 mL of 0.50 M HEDP, then stirring for 168 h at 80 °C.

Characterization: Instrumental analysis. Fourier transform infrared (FT-IR) spectra were taken on a PerkinElmer Spectrum 65 spectrometer. The PANalytical X'Pert Pro X-ray powder diffraction system was used to obtain X-ray diffraction (XRD) patterns. Scanning electron microscopy (SEM) images and energy dispersive X-ray spectroscopy (EDS) were obtained from a Zeiss Supra 55 VP field emission SEM at City College. Specific surface area (SSA) measurements were made using a Micromeritics Tristar 3000 surface area and porosity analyzer. Inductively coupled plasma-optical emission spectrometry (ICP-OES) analyses were carried out on acid digested HAP and mHAP samples as well as on metal ion solutions on a PerkinElmer Optima 7000 DV ICP-OES.The thermogravimetric analysis (TGA) was carried out on a TA Instruments SDTQ600 analyzer. Twenty mg of each solid was used for each analysis. Heat flow and weight changes associated with transitions and reaction-involved materials over the ambient-to-1000 °C temperature range (heating rate of 5 °C/min) under air atmosphere (100 mL/min) were measured simultaneously.

^{31}P NMR measurements were carried out with a Bruker ADVANCE 400 apparatus. The experimental conditions were 10 kHz and room temperature (20−25 °C).

Effect of pH. HAP and mHAP (0.25 g) were stirred in 50 mL of 0.10 M NaOH also containing 2.5 g of NaCl for 17 h to determine their acid capacities. The mixture was filtered, and the filtrate was titrated with 0.10 M HCl to calculate the level of HEDP incorporation.

The effect of pH on stability and solubility was determined by measuring the concentration of calcium released into solution by contacting 20 mL of 0.10 M KNO_3 with 0.10 g of HAP or mHAP5A for 1 or 24 h at pH values adjusted between 2 and 8 with KOH or HNO_3.

Elemental Analysis. Samples were digested in acid in order to determine their organic and inorganic phosphorus capacities.[47] The organic phosphorus capacity was measured by dissolving 20 mg of HAP or mHAP in 10 mL of hot concentrated sulfuric acid in the presence of copper sulfate and potassium persulfate. For inorganic phosphate measurements, 0.10 M HCl was the sole reagent. Digested samples were neutralized, combined with a vanadate-molybdate reagent to produce a yellow complex and analyzed with a Spec 21 instrument. The vanadate−molybdate reagent was prepared by combining 2.50 g of ammonium heptamolybdate tetrahydrate in 30 mL of water to 0.128 g of ammonium metavanadate in 30 mL of water also containing 3.3 mL of concentrated HCl in a 100 mL volumetric flask, which was then diluted to the mark with water.[48] The percent phosphorus contributed by HEDP was calculated using eq 1.

$$\%P_{org} = (P_T - P_{inorg})/P_T \times 100 \quad (1)$$

where P_T is the total phosphorus capacity and P_{inorg} is the inorganic phosphorus capacity.

EDS determined the amounts of calcium and phosphorus to calculate Ca/P ratios. These values were compared to those from ICP measurements of acid-digested samples.

Metal Ion Sorption. Binding affinities were measured for HAP and mHAP: 0.10 g were shaken with separate 10^{-4} N nitrate solutions of Cu^{2+}, Ni^{2+}, Zn^{2+}, Cd^{2+}, and Pb^{2+} for 5 h. To determine their selectivity in the presence of competing nontoxic ions, the solutions were also prepared containing 1 N $Ca(NO_3)_2$. HAP and mHAP were contacted at ambient temperature (20 ± 2 °C) for 5 h followed by centrifugation and microsyringe filtration (0.45 μm pore). HAP-free metal ion solutions were analyzed as controls.

RESULTS

The modified HAPs were characterized by a diverse set of instrumental analyses.

DOI: 10.1021/ie504181z
Ind. Eng. Chem. Res. 2015, 54, 585−596

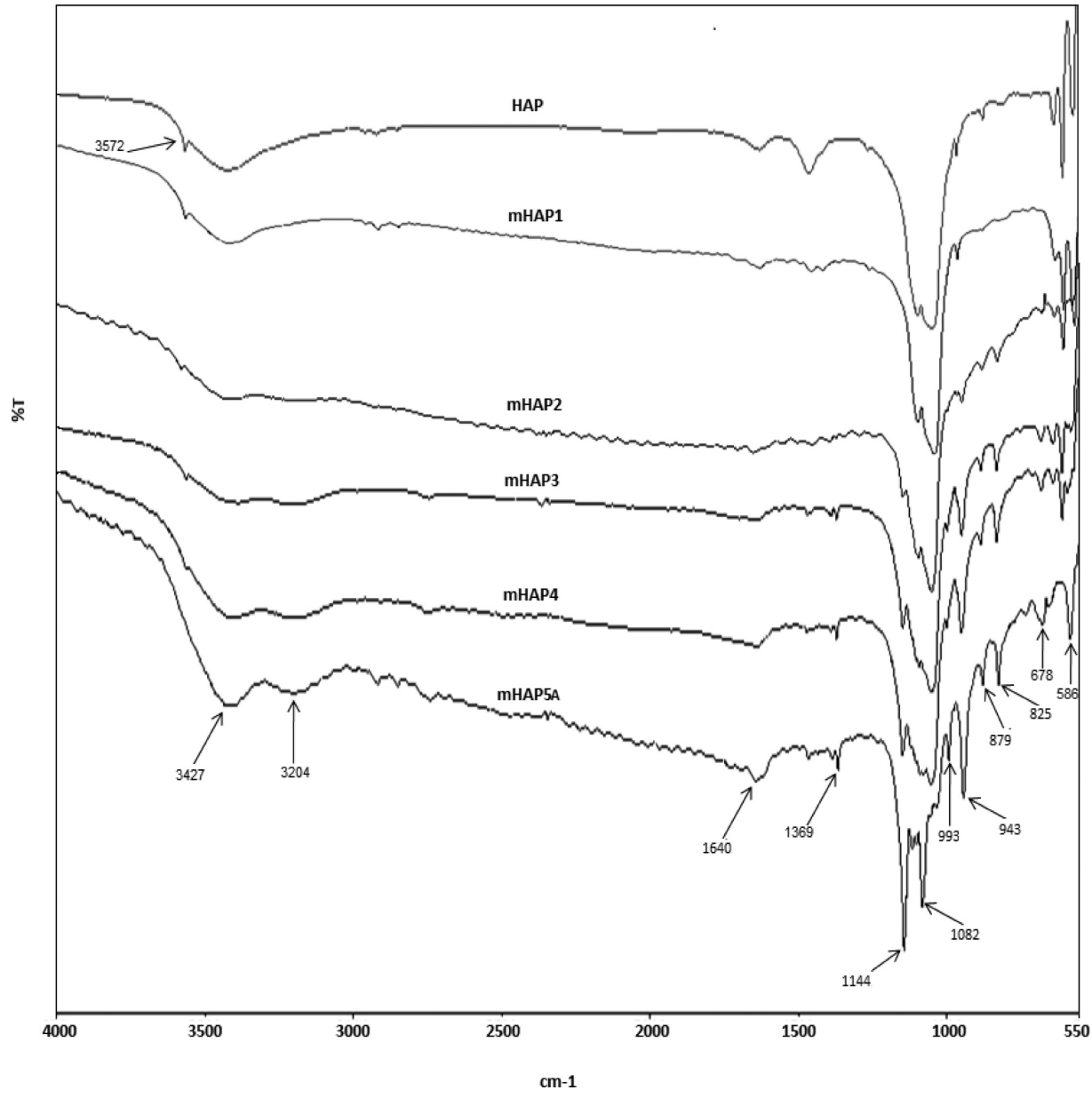

Figure 1. FT-IR spectra of HAP, and HAP modified at 80 °C for 168 h using 0.01 M (mHAP1), 0.05 M (mHAP2), 0.10 M (mHAP3), 0.20 M (mHAP4), and 0.50 M (mHAP5A) HEDP.

FT-IR. HAP was initially modified with 0.01, 0.05, 0.10, 0.20, and 0.50 M HEDP for 168 h at 80 °C (mHAP1−5A, Table 1). As the concentration of HEDP increased, there was a gradual split in the phosphate band between 1082 and 1144 cm^{-1} as well as a new band at 993 cm^{-1}. The intensity of the bands at 943, 879, and 825 cm^{-1} also increased with increasing HEDP concentration and the free −OH band (3572 cm^{-1}) disappeared while a new band for intermolecular H-bonds appeared at 3204 cm^{-1} (Figure 1). Modification was most pronounced with 0.50 M HEDP (mHAP5A), and this concentration was used for all subsequent modifications.

Low temperature (20 °C) and high temperature (80 °C) conditions were combined with reaction times of 4, 168, and 720 h to generate six different mHAPs (mHAP5A−C and mHAP6A−C, Table 1). HAPs modified at 80 °C or long reaction times (168 and 720 h) showed the phosphate band split (Figure 2 and Supporting Information, Figure S1). mHAP6B (4 h/20 °C) showed no band split and had a spectrum very similar to HAP itself (Figure 1) as did cHAP (Supporting Information, Figure S2). When sHAP1 was modified with HEDP for 168 h at 80 °C, the new sHAP2 had a spectrum similar to mHAP5A but with a slightly broader phosphate band at 1083 cm^{-1} (Figure S2).

XRD. HAP modified at 80 °C showed a new diffraction pattern when compared to unmodified HAP (Figure 3): reaction times of 168 h (mHAP5A) and 720 h (mHAP5C) produced sharper peaks indicating more crystallinity with no significant difference between them. At low temperature, new diffraction patterns were seen only in mHAP6A (168 h) and mHAP6C (720 h) (Supporting Information, Figure S3). The XRD pattern of mHAP6B (4 h) was the same as HAP. mHAP6A and mHAP6C had XRD patterns similar to mHAP5B (Figure 3) indicating that crystallinity was favored at high temperature and long reaction time. There was no difference when comparing the XRD patterns of mHAPs from that of the two long reaction times at high and low

DOI: 10.1021/ie504181z
Ind. Eng. Chem. Res. 2015, 54, 585−596

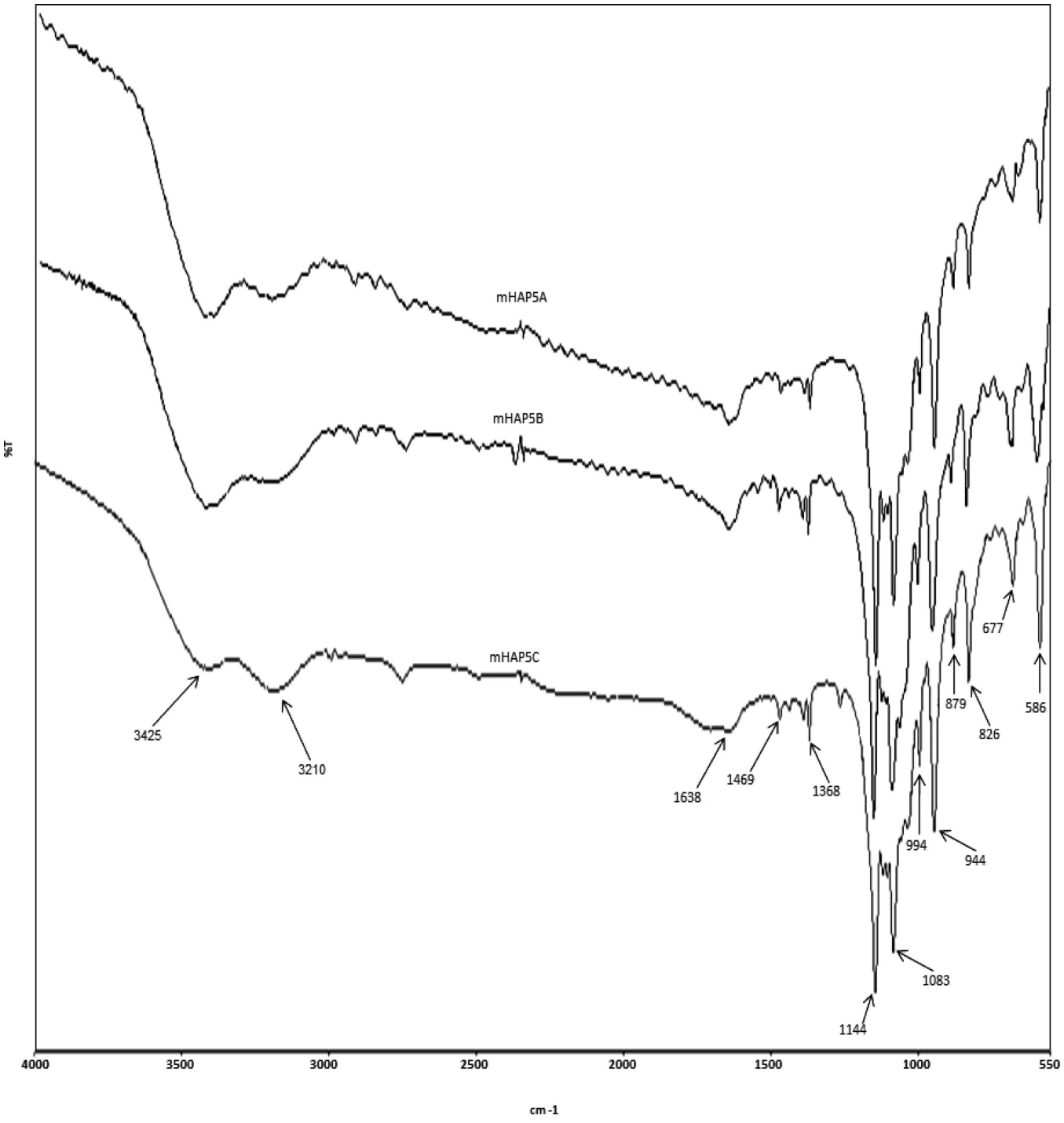

Figure 2. FT-IR spectra of HAP modified with 0.50 M HEDP at 80 °C for 168 h (mHAP5A), 4 h (mHAP5B), and 720 h (mHAP5C).

temperatures. The diffraction pattern of mHAP5A was similar to that of mHAP5C (Figure 3) and mHAP6A resembled mHAP6C (Supporting Information, Figure S3). Given that, subsequent analyses at the long reaction time were limited to the mHAP5A and mHAP6A conditions.

The XRD of cHAP revealed that in the absence of HEDP, no modification of the HAP crystal occurred even when the HAP was exposed to high temperature (80 °C) and long reaction time (168 h) (Figure 4). sHAP1 had a diffraction pattern similar to HAP and cHAP but was more crystalline. This crystallinity did not affect the modification since the XRD pattern of sHAP2 had peaks identical to those for mHAP5A. The only difference was in the extent of crystallinity. Results show the same modification can occur at 168 h/80 °C regardless of the initial Ca/P ratio.

SEM. SEM revealed a microbead structure in the low temperature mHAPs consistent with the SEM of HAP.[49] There was also a trace appearance of a new particle morphology ("strands") within mHAP6A and mHAP6B suggesting a new phase at low levels (Figure 5). The strands were most evident and homogeneously distributed in mHAP5A and mHAP5B, both modified at 80 °C. Modification is confirmed by XRD patterns and FT-IR spectra for all mHAPs except mHAP6B which appeared identical to HAP even though SEM images

DOI: 10.1021/ie504181z
Ind. Eng. Chem. Res. 2015, 54, 585−596

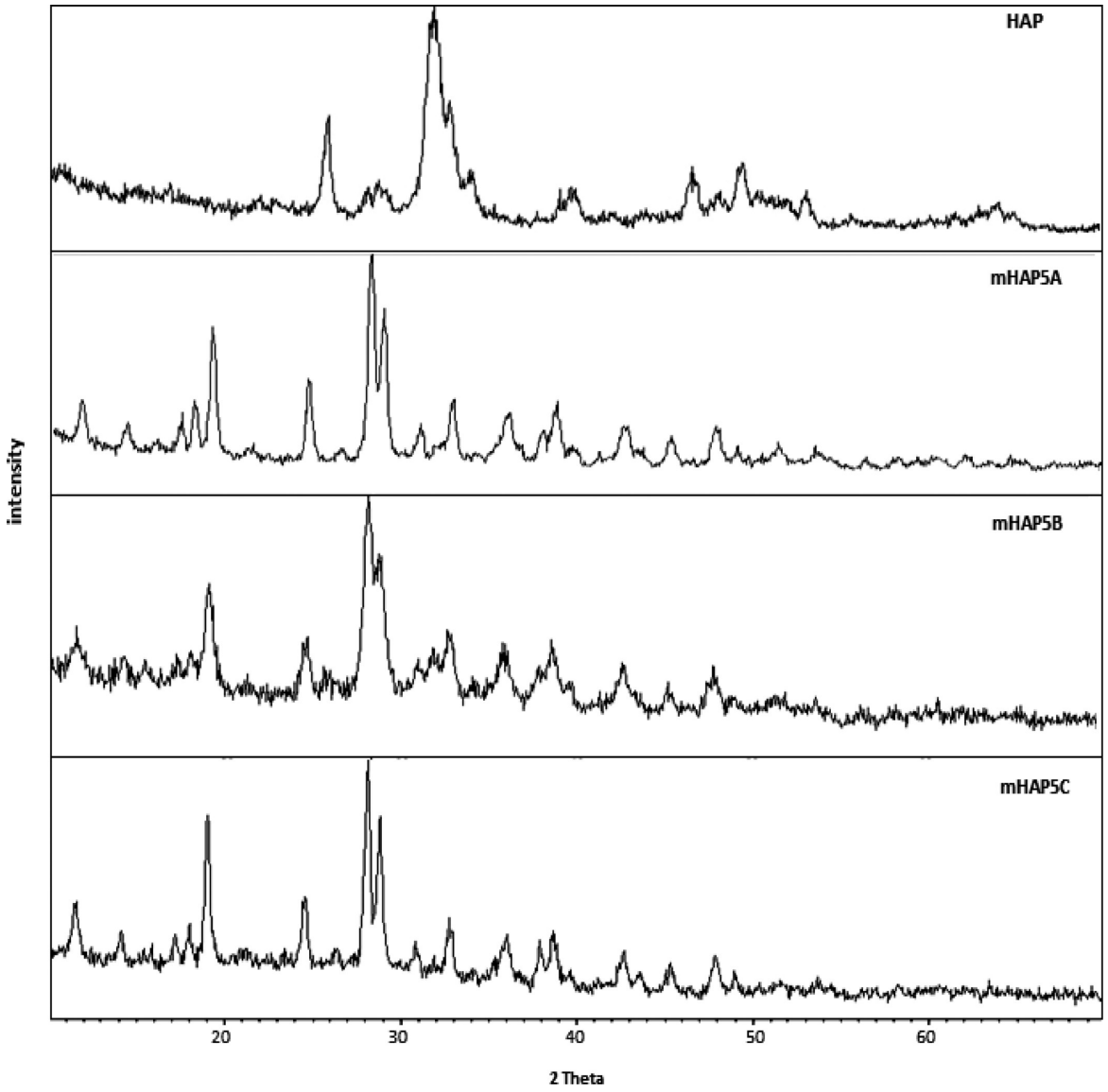

Figure 3. XRD patterns of HAP and HAP modified with 0.50 M HEDP at 80 °C for 168 h (mHAP5A), 4 h (mHAP5B), and 720 h (mHAP5C).

revealed the new phase within it. All three analyses, however, supported an increasing level of modification at higher temperature and longer reaction time.

Specific Surface Area. mHAP5A–B (80 °C reaction) had low SSA compared to HAP and mHAP6A–B (20 °C reaction) (Supporting Information, Table S1). The disappearance of microbeads in high temperature mHAPs and the emergence of continuous strands may account for the SSA decrease.

Effect of pH: Acid Capacity. The acid capacities of HAP, mHAP, and cHAP are affected by reaction time, temperature, and the presence of HEDP (Supporting Information, Table S2): the higher the reaction temperature is (mHAP5A–B), the greater is the acid capacity. Longer reaction times led to higher acid capacities (mHAP5A and mHAP6A) compared to shorter times (mHAP5B and mHAP6B). In the absence of HEDP, the control HAP (cHAP) contacting water for 168 h at 80 °C showed no difference in its acid capacity compared to HAP, which indicates HEDP modification is evident by acid capacity.

Effect of pH: Calcium solubility/stability. The effect of pH on particle stability was determined by placing HAP and mHAP5A in 0.10 M KNO_3. Both dissolved and released high levels of calcium (1.6–2.1 mmol/g) at pH 2, (Figures 6 and 7) and lower levels at pH 4 and 6. However, they behaved differently when placed in solutions at pH 8: HAP released a low level of calcium, as expected since it is known to be stable at high pH,[50] but mHAP5A released almost as much Ca^{2+} as it did at pH 2. This is discussed in the subsequent section.

Phosphorus Analysis. The percent organic phosphorus in the mHAPs was measured by using 0.10 M HCl to dissolve the inorganic phosphate and concentrated H_2SO_4 to dissolve inorganic and organic phosphates.[47] The amount of organic phosphate relative to inorganic phosphate was high at long reaction time (mHAP5A and mHAP6A, Table 2) and lower at short reaction time (mHAP5B and mHAP6B). The same trend was seen at high temperature (mHAP5A–B) and low temperature (mHAP6A–B).

The $\%P_{org}$ calculated in Table 2 for each mHAP gives the amount of organic P relative to the total P, not the wt % P per gram mHAP. Table 3 shows the wt % of HEDP for mHAP5A, mHAP5B, mHAP6A, and mHAP6B. These calculations are consistent with the FT-IR spectra (Figure 2 and Supporting Information, Figure S1) which reveal new bands for mHAP5A,

DOI: 10.1021/ie504181z
Ind. Eng. Chem. Res. 2015, 54, 585–596

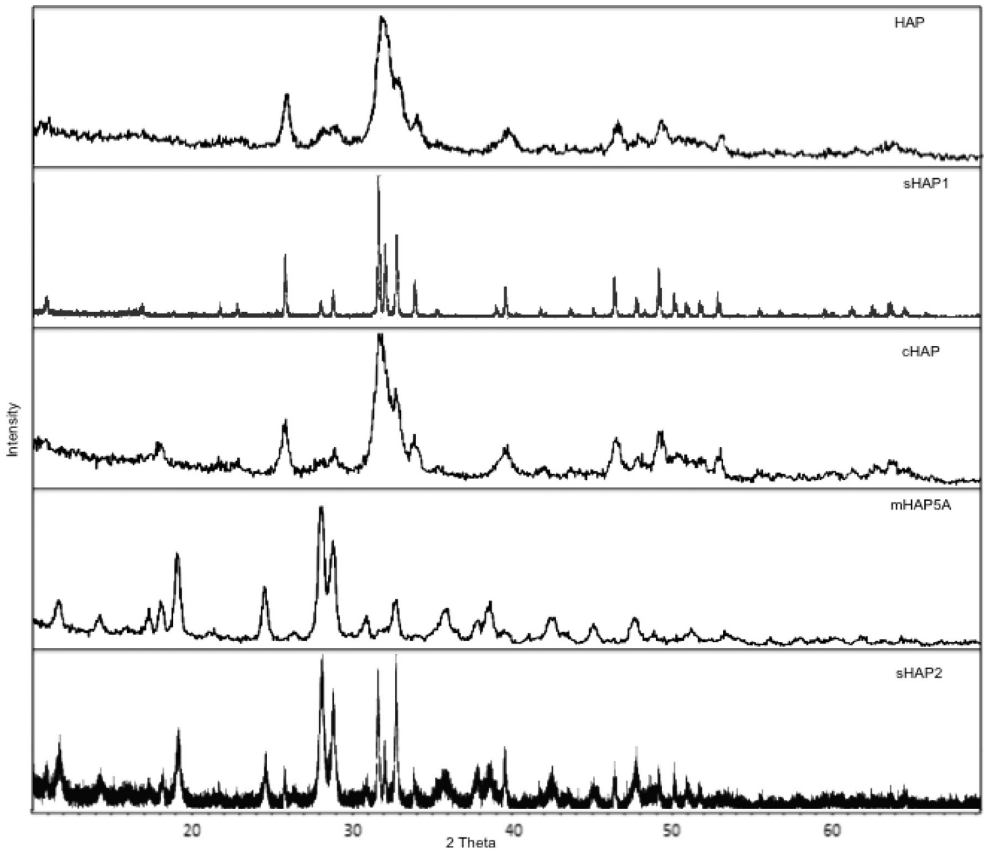

Figure 4. XRD of HAP, stoichiometric HAP (sHAP1), HAP contacted in H_2O for 168 h at 80 °C (cHAP), HAP modified with 0.50 M HEDP for 168 h at 80 °C (mHAP5A), and stoichiometric HAP modified with 0.50 M HEDP for 168 h at 80 °C (sHAP2).

mHAP5B, and mHAP6A, but not for mHAP6B which, with 5.7 wt % of HEDP, is at the detection limit for FT-IR.

The elemental analysis suggests that for mHAP5A, mHAP5B, and mHAP6A, the modification is more than a surface phenomenon. This is consistent with the acid capacities for mHAP5A, mHAP5B, and mHAP6A which were also greater than the amount that could be reasonable for only surface modification. mHAP5A, with 100% P_{org}, is therefore indicative of HAP modified in the bulk phase and mHAP6B, with 10.6% P_{org}, may be only surface modified.

^{31}P NMR. ^{31}P NMR spectra were obtained for mHAP, mHAP6B, mHAP5B, mHAP6A, and mHAP5A (Figure 8). The peak at 3 ppm arises from the inorganic P in HAP.[51] As reaction time and temperature increase, this peak decreases and a new peak at 19 ppm emerges due to HEDP.[52] The sample modified for 4 h at 20 °C (mHAP6B) has a spectrum that is almost identical to unmodified HAP indicating little HEDP present. mHAP5A, modified for the longest time (168 h) and the highest temperature (80 °C), only has a peak corresponding to HEDP. All other samples have mixed phases. These results are consistent with the elemental analysis.

Thermogravimetric Analysis. HAP and mHAP were heated to 1000 °C at 20 °C/min under air atmosphere in order to determine the weight loss (%) resulting from the incorporated HEDP (Supporting Information, Figure S4). The decline in weight occurred between 400 and 700 °C after the loss of water, with the greatest loss evident between 400 and 570 °C. HAP and mHAP6B (4 h/20 °C) had the least weight loss, 5.6% and 5.8%, respectively (Supporting Information, Table S3). Weight loss increased to 20.7% at longer reaction times (168 h/20 °C, mHAP6A), but an increase in temperature (4 h/80 °C, mHAP5B) resulted in a loss of only 12.3%. The temperature range and weight loss values are consistent with what has been observed in similar systems; for example, a 10% weight loss has been found for di(2,4,4-trimethylpentyl)phosphinic acid sorbed within clay.[53] A longer reaction time thus allows more HEDP incorporation than a higher temperature. This is consistent with the P-elemental results, wherein mHAP6A had 52.1% HEDP compared to mHAP5B with 32.6%. mHAP5A modified for 168 h/80 °C was expected to show the highest mass loss but it had a mass loss of only 14.8%, which is not consistent with its P-elemental result since it had the most HEDP. This is likely tied to its morphology and requires further study.

Calcium−HEDP. Calcium−HEDP was synthesized by contacting $Ca(OH)_2$ with HEDP. FT-IR spectra (Figure 9) revealed that Ca−HEDP was different from mHAP5A and more closely resembled unmodified HAP. Phosphate bands contributed by HEDP appeared at 944 cm^{-1} for Ca−HEDP and mHAP5A, as seen from the FT-IR of HEDP alone (Figure 9).

EDS and ICP. EDS showed a decreasing Ca/P ratio with increasing reaction time and temperature. Results by ICP were consistent with EDS measurements. A decreased Ca/P ratio was associated with a higher P content corresponding to HEDP incorporation into the HAP (Table 4).

Metal Ion Studies. The metal ion affinities of four mHAPs: mHAP6B (4 h at 20 °C), mHAP5B (4 h at 80 °C), mHAP6A (168 h at 20 °C), and mHAP5A (168 h at 80 °C) were determined by contacting them with lead(II) nitrate solutions.

DOI: 10.1021/ie504181z
Ind. Eng. Chem. Res. 2015, 54, 585−596

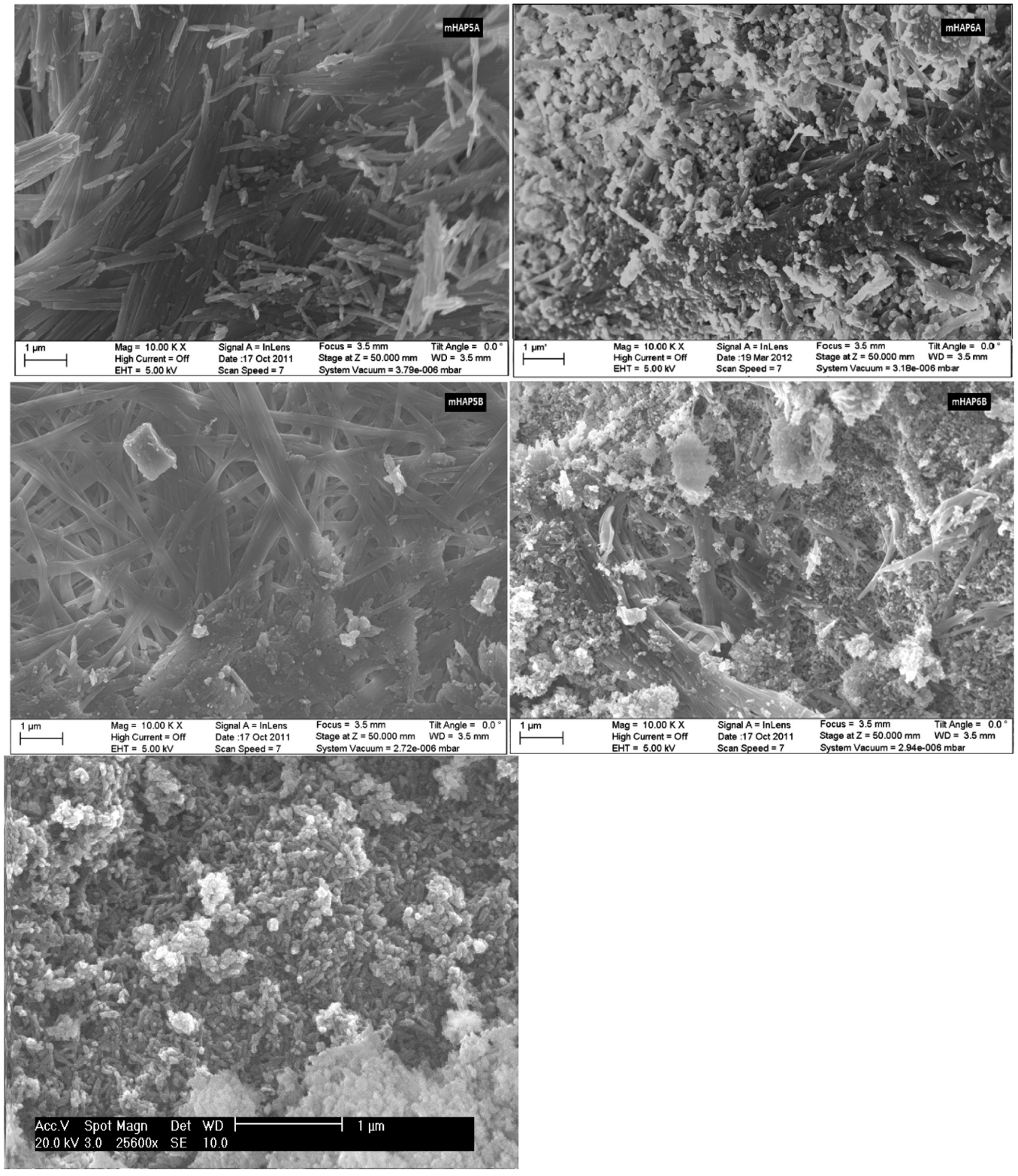

Figure 5. SEM of HAP modified with 0.50 M HEDP at 80 °C for 168 h (mHAP5A), 4 h (mHAP5B), and at 20 °C for 168 h (mHAP6A) and 4 h (mHAP6B) as well as HAP itself (bottom left).

Sorption of Pb^{2+} was highest for mHAP6B, decreased for mHAP5B and mHAP6A, then increased for mHAP5A (Supporting Information, Figure S5).

Sorption by mHAP6B and mHAP5A was studied in more detail by contacting them with nitrate solutions of Cu^{2+}, Ni^{2+}, Zn^{2+}, and Cd^{2+} (Figure 10). HAP and mHAP6B removed all metal ions from solution with high efficiency (>85%) but showed no selectivity. mHAP5A, however, removed high levels of Pb^{2+} (90%) and Cd^{2+} (82%) but <25% of the other metal ions. (No Cu^{2+} was removed by mHAP5A.) Its selectivity was tested in a solution containing a high level of calcium (1 N), where the presence of calcium simulates a nontoxic, aqueous

DOI: 10.1021/ie504181z
Ind. Eng. Chem. Res. 2015, 54, 585−596

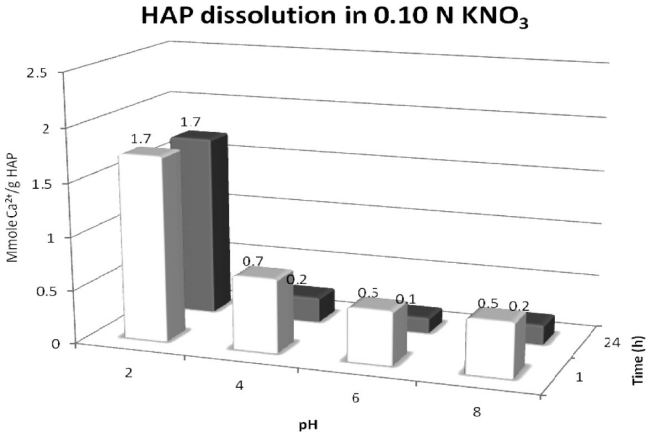

Figure 6. Calcium release for HAP in KNO_3 solutions at pH 2, 4, 6, and 8 at 1 and 24 h contact.

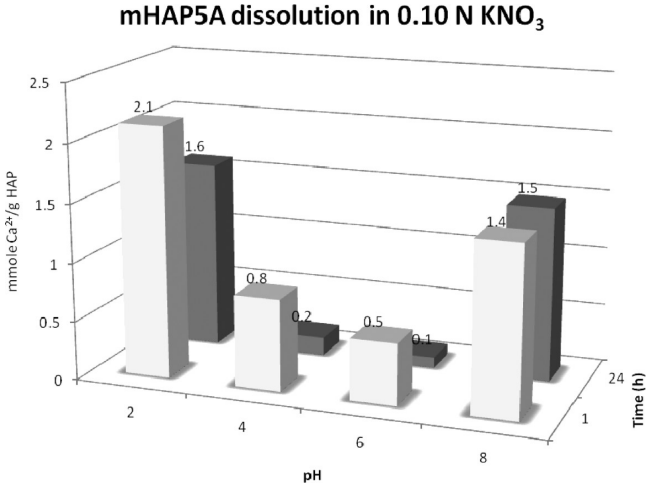

Figure 7. Ca^{2+} release for mHAP5A in KNO_3 solutions at pH 2, 4, 6, and 8 at 1 and 24 h contact.

Table 2. Phosphorus Elemental Analysis of HAP and mHAP

HAP	P_T (mmol/g)	P_{inorg} (mmol/g)	$\%P_{org}$ [a]
HAP	5.23	5.21	0.3
mHAP5A	5.97	0	100
mHAP5B	5.63	2.47	56.8
mHAP6A	5.34	0.28	94.8
mHAP6B	5.26	4.70	10.6

[a] $\%P_{org}$ = amount of organic P relative to the total P × 100.

Table 3. Phosphorus wt % in mHAP

	P_{org} (mmol/g)	P_{org} in mHAP (g/g)	P_{org} in mHAP (wt %)	HEDP in mHAP (wt %)
mHAP5A	5.97	0.185	18.5	61.4
mHAP5B	3.16	0.098	9.8	32.6
mHAP6A	5.06	0.157	15.7	52.1
mHAP6B	0.56	0.017	1.7	5.7

environment. Sorption for Pb^{2+} was still high (89%) though Cd^{2+} decreased (16%). HAP also showed decreased metal ion sorption in high calcium concentration for Ni^{2+}, Zn^{2+}, and Cd^{2+} (Figure 11). That HAP retains a high affinity for Pb^{2+} and Cu^{2+} while mHAP5A is selective for Pb^{2+} points to an important

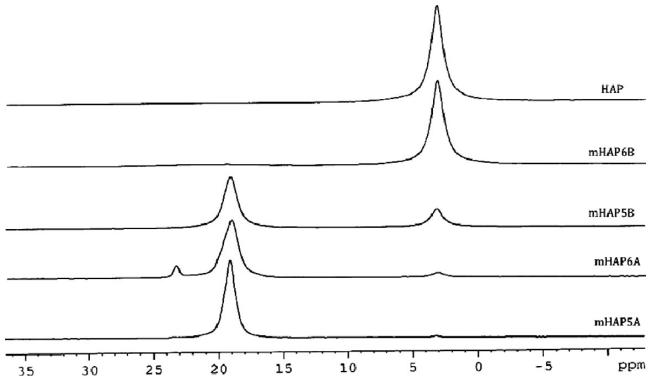

Figure 8. ^{31}P NMR of unmodified HAP, HAP modified with 0.5 M HEDP at 20 °C for 4 h (mHAP6B), 80 °C for 4 h (mHAP5B), 20 °C for 168 h (mHAP6A), and 80 °C for 168 h (mHAP5A).

difference in their sorption mechanism and this is discussed in the next section.

DISCUSSION

Reaction Time and Temperature. HAP has been modified by varying HEDP concentration, reaction time, and reaction temperature. New phosphate bands appeared in the FT-IR spectra at 943, 993, 1082, and 1144 cm^{-1} as HEDP concentration increased. This was seen in high temperature modifications for short and long reaction times (Figure 2) and the low temperature modification for the long reaction time (Supporting Information, Figure S1). FT-IR spectra of both high temperature reactions were identical. At a low reaction temperature and short reaction time, mHAP6B had no change in its FT-IR spectrum compared to HAP. Comparing Figures 1 and 9 leads to the conclusion that the bands at 1082 and 1144 cm^{-1} are due to the P−O stretch of HEDP and the band at 943 cm^{-1} is due to the interaction between P−O and Ca^{2+} in the HAP. The new bands at 825, 879, and 993 cm^{-1} are very weak and so can only be assigned to weak interactions between the HAP and HEDP since they are not present in either of the individual pure spectra. However, SEM images revealed the presence of HAP−HEDP strands and so the amount of HEDP incorporated may be too low at 5.7 wt % to be detected by FT-IR. High temperature and long reaction time both have an effect on HEDP incorporation and the combined effect is pronounced. The acid and phosphorus capacities indicate that there is more than surface modification and HEDP is within the HAP crystal.

Instrumental and Elemental Analyses. ^{31}P NMR and FT-IR gave consistent results. The spectra of mHAP6B were the same as HAP even though the presence of HEDP was evident by elemental analysis (5.7 wt % P). The disappearance of the free −OH band (3572 cm^{-1}) initially present in HAP and the emergence of an intermolecular hydrogen-bond stretch at 3204 cm^{-1} in the other mHAPs suggest that −OH groups in HAP react with HEDP in the modification reaction.

A phosphorus elemental analysis was used to distinguish the organic from inorganic phosphorus in the mHAPs and to quantify the extent of HAP modification with HEDP. The higher is the organic phosphorus capacity, the more HEDP is incorporated into HAP. There was a significant increase in the amount of HEDP measured in mHAP5A (61.4 wt %) prepared at high temperature and long reaction time compared to that in mHAP6B (5.7 wt %) prepared at low temperature and short

DOI: 10.1021/ie504181z
Ind. Eng. Chem. Res. 2015, 54, 585−596

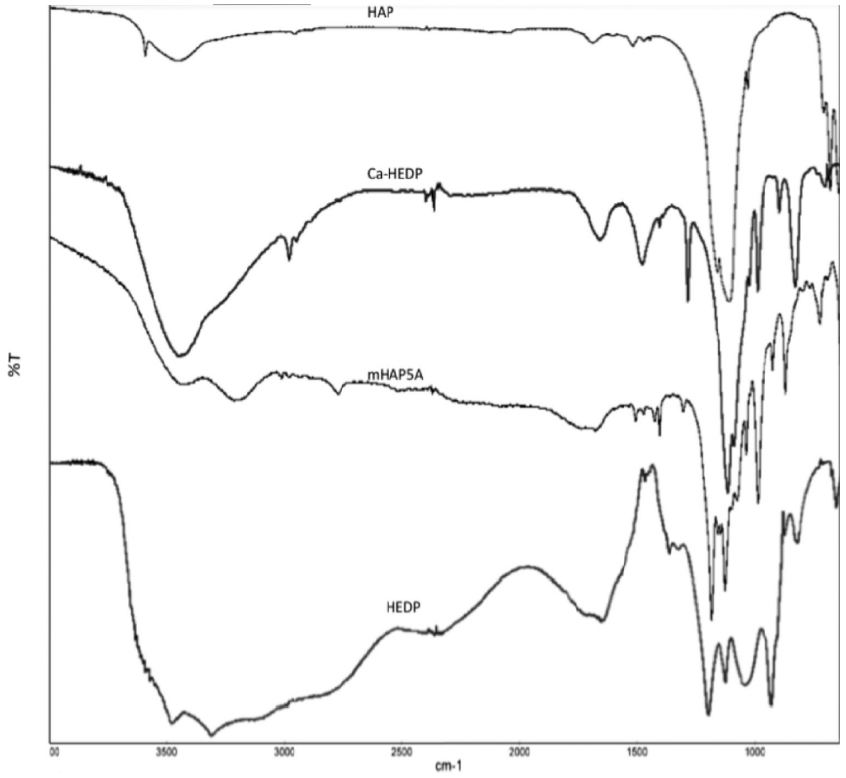

Figure 9. FT-IR of HAP, a calcium salt of HEDP (Ca−HEDP), HAP modified with 0.50 M HEDP for 168 h at 80 °C (mHAP5A) and HEDP alone.

Table 4. Analysis of Calcium to Phosphorus Ratio

	Ca/P ratio (EDS)	Ca/P ratio (ICP)
HAP-700	1.51	1.52
mHAP5A	0.50	0.55
mHAP5B	0.56	0.58
mHAP6A	0.54	0.59
mHAP6B	1.45	1.21

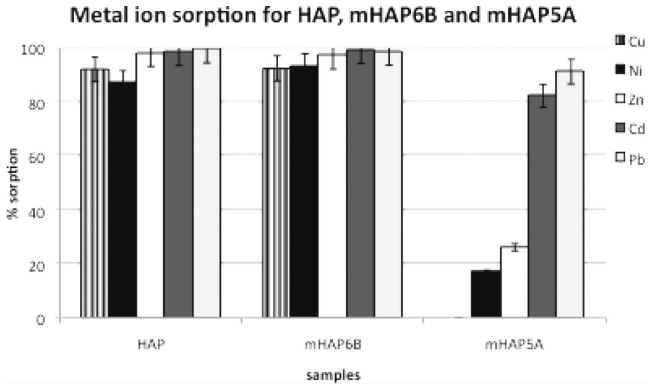

Figure 10. Metal ion sorption for HAP, mHAP6B, and mHAP5A in nitrate solutions of Cu(II), Ni(II), Zn(II), Cd(II), and Pb(II).

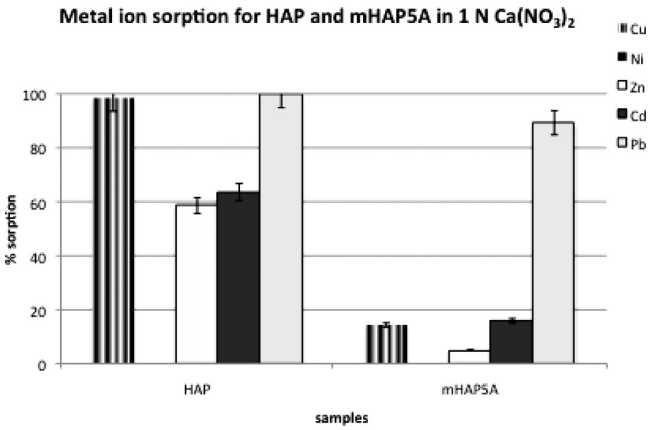

Figure 11. Metal ion sorption for HAP and mHAP5A in nitrate solutions of Cu(II), Ni(II), Zn(II), Cd(II), and Pb(II) with 1 N $Ca(NO_3)_2$.

reaction time (20 °C/4 h). mHAP6A and mHAP5B, prepared at low temperature/long time and high temperature/short time, respectively, give HEDP levels of 52.1% and 32.6%, respectively, with the higher amount appearing at long reaction time. These results complement the instrumental analysis and confirm that high temperature/long reaction time allows the most HEDP to be incorporated into HAP.

New diffraction patterns and sharp XRD peaks indicate an increase in crystallinity of the HAP modified for the long reaction time at high temperature. mHAPs produced by other conditions did not have the same high extent of crystallinity. SEM images of the mHAPs distinguished between HAP microbeads and HEDP-modified strands. EDS analysis showed that the strands had more phosphorus (i.e., a lower Ca/P ratio) than samples containing more microbeads. The microbeads are expected to have a greater surface area than strands and this accords with data which showed a lower SSA for samples with more strands (mHAP5A−B) and a higher SSA for samples with more microbeads (mHAP6A−B).

FT-IR spectra confirmed that mHAP5A was similar to modified stoichiometric HAP (sHAP2) but different from the calcium salt of HEDP produced with $Ca(OH)_2$ and HEDP in

DOI: 10.1021/ie504181z
Ind. Eng. Chem. Res. 2015, 54, 585−596

the absence of phosphoric acid. XRD provides further support. Browning and Fogler prepared Ca−HEDP salts with different Ca/HEDP ratios and studied their XRDs.[54] The Ca−HEDP salt having a 1:1 Ca/HEDP ratio gave four distinct peaks at 7, 12, 16, and 17 degrees. As the ratio of Ca to HEDP increased, the XRDs showed a more amorphous structure. A comparison of Figures 3 and 12 confirms that mHAP5A is different from Ca−HEDP.

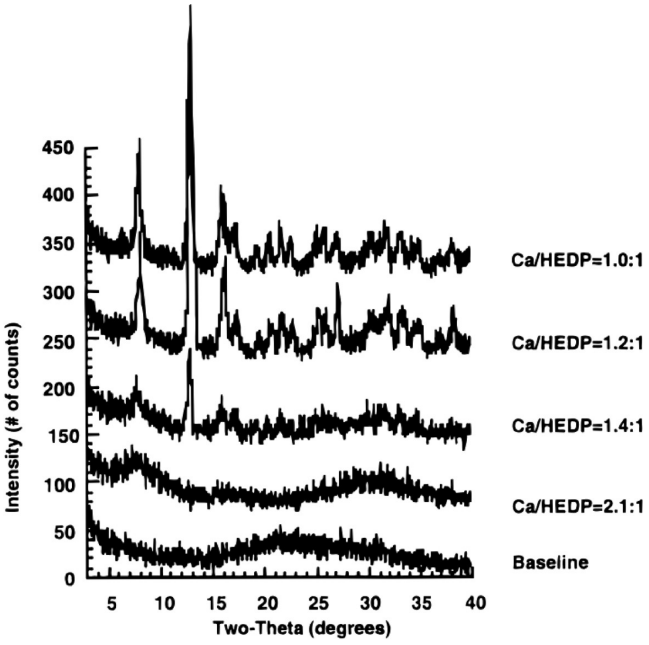

Figure 12. XRD of calcium−HEDP salts of different Ca/HEDP ratios.[53] Reprinted from ref 54. Copyright 1996 American Chemical Society.

Metal Ion Studies. Modified HAP behaved differently from HAP during pH equilibration and metal ion sorption studies. At pH 8, mHAP5A released high levels of Ca^{2+} compared to HAP. This can be explained by noting that mHAP5A required the addition of a higher amount of KOH to raise the pH and the resulting high concentration of K^+ forced ion exchange with Ca^{2+}. Although the complexation constant for potassium−HEDP is significantly lower (log K = 1.8)[45] than that of calcium−HEDP (log K = 6.4),[45] these values derive from measurements with equal concentrations of K^+ and Ca^{2+}. At very high K^+/Ca^{2+} ratios, the law of mass action favors potassium−HEDP and causes Ca^{2+} to be released into solution.

mHAP5A removed Pb^{2+} and Cd^{2+} from nitrate solutions with high efficiency compared to the sorption of other divalent ions (Pb^{2+} > Cd^{2+} > Zn^{2+} > Ni^{2+} > Cu^{2+}). These results were comparable to those for the commercially available extractant di(2-ethylhexyl)phosphoric acid.[55] Its affinity for Pb^{2+} (90%) and Cd^{2+} (60%) are as high as found for HEDP, while sorption of Ni^{2+} and Cu^{2+} is lowest. There was no selectivity among metal ions for mHAP6B, confirming that the increased levels of HEDP in mHAP5A strongly correlate with its metal ion affinities.

In a background of 1 N Ca^{2+} ions, mHAP5A retained its selectivity for Pb^{2+} while its affinity for Cd^{2+} decreased; HAP also retained its high affinity for Pb^{2+} but had a high affinity for Cu^{2+} as well. This disparity in behavior between mHAP5A and HAP is due to HAP operating via a relatively nonselective electrostatic ion-exchange mechanism while mHAP5A is operating via a mechanism in which there is significant coordination that allows for metal−ligand covalency. Coordination implies a correlation with the polarizabilities of the metal ions and this is the case here. The Misono softness parameter quantifies metal ion polarizabilities[56] and has been used successfully to explain the affinities of polymer-supported phosphate ligands.[57] The ions studied have the values 0.40 (Pb^{2+}), 0.30 (Cd^{2+}), 0.28 (Cu^{2+}), 0.25 (Ni^{2+}), and 0.24 (Zn^{2+}). The degree to which the softness parameter agrees with the sorption results suggests that complexants operating by coordinating to metal ions will retain that mechanism once bound within HAP. This widens the applicability of the technique described in this report by allowing a match between a given application and the complexant to be bound within HAP. Further studies are in progress.

CONCLUSION

The aim of this study is to develop a technique whereby HAP can be modified with ion-selective complexants and used in groundwater remediation. This initial report establishes the feasibility of the technique. HEDP can be incorporated into HAP and the metal ion affinities expected from solvent extraction studies are maintained indicating that immobilization within the inorganic matrix does not affect its binding mechanism. Subsequent studies will show how mHAP5A can be fabricated as a membrane used to sorb metal ions that contaminate water, then thermally decomposed after sorption, leaving the toxic metal immobilized within the purely inorganic HAP for subsequent valorization. Furthermore, it is important to note that the polar nature of the complexants permits binding to molecules of importance in wastewater treatment. Such molecules include estrogens and other hormones, endocrine disruptors, polyphenols, dyes and antibiotics. As with metal ions, the polar complexants incorporated into the HAP will permit the selective removal of the targeted compound.

ASSOCIATED CONTENT

Supporting Information

Figure S1, FT-IR spectra HAP modified with 0.50 M HEDP at 20 °C, for 168 h (mHAP6A), 4 h (mHAP6B) and 720 h (mHAP6C); Figure S2, FT-IR of HAP, stoichiometric HAP (sHAP1), HAP contacted in H2O for 168 h at 80 °C (cHAP), HAP modified with 0.50 M HEDP for 168 h at 80 °C (mHAP5A), and stoichiometric HAP modified with 0.50 M HEDP for 168 h at 80 °C (sHAP2); Figure S3, XRD patterns of HAP and HAP modified with 0.50 M HEDP at 20 °C, for 168 h (mHAP6A), 4 h (mHAP6B), and 720 h (mHAP6C); Table S1, specific surface areas for HAP and mHAP; Table S2, acid capacities of HAP and mHAP; Figure S4, thermogravimetric curves for HAP and mHAP heated to 1000 °C at 20 °C/min; Table S3, thermogravimetric analysis for HAP and mHAP; Figure S5, Pb(II) ion sorption for HAP modified with 0.50 M HEDP for 4 h at 20 °C (mHAP6B), 4 h at 80 °C (mHAP5B), 168 h at 20 °C (mHAP6A), and 168 h at 80 °C (mHAP5A). This material is available free of charge via the Internet at http://pubs.acs.org.

AUTHOR INFORMATION

Corresponding Author

*E-mail: alexsd@hunter.cuny.edu.

DOI: 10.1021/ie504181z
Ind. Eng. Chem. Res. 2015, 54, 585−596

Notes

The authors declare no competing financial interest.

■ ACKNOWLEDGMENTS

We gratefully acknowledge support from the Minority Biomedical Research Support RISE (MBRS-RISE) program at Hunter College (Grant No. GM060665) for graduate funding to Y.D. We are also grateful for support from the Chemical Sciences, Geosciences and Biosciences Division, Office of Basic Energy Sciences, Office of Science, U.S. Department of Energy, through Grant DE-FG02-02ER15287.

■ REFERENCES

(1) Narasaraju, T. S. B.; Phebe, D. E. Some physico-chemical aspects of hydroxyapatite. *J. Mater. Sci.* **1996**, *31*, 1−21.
(2) Lim, G.K.; Wang, J.; Ng, S. C.; Chew, C. H.; Gan, L. M. Processing of hydroxyapatite via microemulsion and emulsion routes. *Biomaterials* **1997**, *18*, 1433−1439.
(3) Sanosh, K. P.; Chu, M. C.; Balakrishnan, A.; Kim, T. N.; Cho, S. J. Preparation and characterization of nano-hydroxyapatite powder using sol-gel technique. *Bull. Mater. Sci.* **2009**, *32*, 465−470.
(4) Qi, C.; Zhu, Y.; Lu, B.; Zhao, X.; Zhao, J.; Chen, F.; Wu, J. Hydroxyapatite hierarchically nanostructured porous hollow microspheres: rapid, sustainable microwave-hydrothermal synthesis by using creatine phosphate as an organic phosphorus source and application in drug delivery and protein adsorption. *Chem.—Eur. J.* **2013**, *19*, 5332−5341.
(5) Hasret, E.; Ipekoglu, M.; Altintas, S.; Ipekoglu, N. A. Microwave-assisted synthesis of hydroxyapatite for the removal of lead(II) from aqueous solutions. *Environ. Sci. Pollut. Res.* **2012**, *19*, 2766−2775.
(6) Manocha, S.; Joshi, P.; Patel, B.; Manocha, L. M. Synthesis and characterization of hydroxyapatite nanoparticles using sol−gel method. *Eurasian ChemTechnol. J.* **2011**, *13*, 85−88.
(7) Ryu, I.; Kim, D.; Han, J.; Lee, M. Influence of two-step sintering variables on phase stability of hydrothermally prepared HAP nano powders. *Key Eng. Mater.* **2008**, 361−363 (Pt. 1, Bioceramics), 91−94..
(8) Charrière, E.; Lemaitre, J.; Zysset, P. Hydroxyapatite cement scaffolds with controlled macroporosity: Fabrication protocol and mechanical properties. *Biomaterials* **2003**, *24*, 809−817.
(9) Liu, D. M. Influence of porosity and pore size on the compressive strength of porous hydroxyapatite ceramic. *Ceram. Int.* **1997**, *23*, 135−139.
(10) Pramanik, S.; Agarwal, A. K.; Rai, K. N.; Garg, A. Development of high strength hydroxyapatite by solid-state-sintering process. *Ceram. Int.* **2007**, *33*, 419−426.
(11) Al-Qasas, N. S.; Rohani, S. Synthesis of pure hydroxyapatite and the effect of synthesis conditions on its yield, crystallinity, morphology, and mean particle size. *Sep. Sci. Technol.* **2005**, *40*, 3187−3224.
(12) Raynaud, S.; Champion, E.; Bernache-Assollant, D.; Thomas, P. Calcium phosphate apatites with variable Ca/P atomic ratio I. Synthesis, characterisation, and thermal stability of powders. *Biomaterials* **2002**, *23*, 1065−1072.
(13) El-Hammari, L.; Marroun, H.; Laghzizil, A.; Saoiabi, A.; Roux, C.; Livage, J.; Coradin, T. Organically modified porous hydroxyapatites: A comparison between alkylphosphonate grafting and citrate chelation. *J. Solid State Chem.* **2008**, *181*, 848−854.
(14) Ivanova, T. I.; Frank-Kamenetskaya, O. V.; Kol'tsov, A. B.; Ugolkov, V. L. Crystal structure of calcium-deficient carbonated hydroxyapatite. Thermal decomposition. *J. Solid State Chem.* **2001**, *160*, 340−349.
(15) Tanaka, H.; Ibaraki, K.; Uemura, M.; Hino, R.; Kandori, K.; Ishikawa, T. Phase transformation of calcium phenyl phosphate in calcium hydroxyapatite. *Mater. Res. Bull.* **2007**, *42*, 1364−1373.
(16) Salas, J.; Benzo, Z.; Gonzalez, G.; Marcano, E.; Gomez, C. Effect of Ca/P ratio and milling material on the mechanochemical preparation of hydroxyapaptite. *J. Mater. Sci: Mater. Med.* **2009**, *20*, 2249−2257.
(17) Aizawa, M.; Ueno, H.; Itatani, K.; Okada, I. Stoichiometry and particle morphology effects on the aptitude to compaction of apatitic structure powders. *J. Eur. Ceram. Soc.* **2006**, *26*, 501−507.
(18) Wang, A.; Liu, D.; Yin, H.; Wu, H.; Wada, Y.; Ren, M.; Jiang, T.; Cheng, X.; Xu, Y. Size-controlled synthesis of hydroxyapatite nanorods by chemical precipitation in the presence of organic modifiers. *Mater. Sci. Eng., C* **2007**, *27*, 865−869.
(19) Yunoki, S.; Ikoma, T.; Monkawa, A.; Marukawa, E.; Sotome, S.; Shinomiya, K.; Tanaka, J. Three-dimensional porous hydroxyapatite/collagen composite with rubber-like elasticity. *J. Biomater. Sci., Polym. Ed.* **2007**, *18*, 393−409.
(20) Hirai, S.; Nishinaka, K.; Shimakage, K.; Uo, M.; Watari, F. Hydroxyapatite coating on titanium substrate by the sol−gel process. *J. Am. Ceram. Soc.* **2004**, *87*, 29−34.
(21) Chen, C.; Oakes, C. S.; Byrappa, K.; Riman, R. E.; Brown, K.; TenHuisen, K. S.; Janas, V. F. Synthesis, characterization, and dispersion properties of hydroxyapatite prepared by mechanochemical−hydrothermal methods. *J. Mater. Chem.* **2004**, *14*, 2425−2432.
(22) Drinking Water Contaminants, List of Contaminants & their MCLs. http://water.epa.gov/drink/contaminants/index.cfm (accessed January 8, 2015).
(23) Pasqui, D.; Torricelli, P.; De Cagna, M.; Fini, M.; Barbucci, R. Carboxymethyl cellulose−hydroxyapatite hybrid hydrogel as a composite material for bone tissue engineering applications. *J. Biomed. Mater. Res. Part A* **2014**, *102*, 1568−1579.
(24) Lu, B.; Zhu, Y.; Chen, F.; Qi, C.; Zhao, X.; Zhao, J. Solvothermal transformation of a calcium oleate precursor into large-sized highly ordered arrays of ultralong hydroxyapatite microtubes. *Chem.−Eur. J.* **2014**, *20*, 7116−7121.
(25) Liu, X.; Lin, K.; Qian, R.; Chen, L.; Zhuo, S.; Chang, J. Growth of highly oriented hydroxyapatite arrays tuned by quercetin. *Chem.−Eur. J.* **2012**, *18*, 5519−5523.
(26) Bailliez, S.; Nzihou, A.; Bernache-Assolant, D.; Champion, E.; Sharrock, P. Removal of aqueous lead ions by hydroxyapatites: Equilibria and kinetic processes. *J. Hazard. Mater.* **2007**, *A139*, 443−446.
(27) Bailliez, S.; Nzihou, A.; Beche, E. B.; Flamant, G. Removal of lead (Pb) by hydroxyapatite sorbent. *Trans. IChemE, Part B* **2004**, *82* (B2), 175−180.
(28) Nzihou, A. Toward the valorization of waste and biomass. *Waste Biomass Valor.* **2010**, *1*, 3−7.
(29) Baldi, G.; Cioni, A.; Dami, V.; Soldi, A.; Signorini, A.; Vincenzini, P.; Dondi, M. Nano-structured glassy and ceramic surfaces: development of "active" materials for an innovative approach to building industry. *Adv. Sci. Technol.* **2011**, *68*, 135−144.
(30) Nzihou, A.; Sharrock, P. Role of phosphate in the remediation and reuse of heavy metal polluted wastes and sites. *Waste Biomass Valor.* **2010**, *1*, 163−174.
(31) Kondo, S.; Groszek, A. J.; Okda, F.; Suzuki, T. The enthalpy of interaction of calcium hydroxyapatite surface with some metal ions. *J. Soc. Inorg. Mater., Japan* **2002**, *9*, 271−275.
(32) Mavropoulos, E.; Rossi, A. M.; Costa, A. M.; Perez, C. A. C.; Moreira, J. C.; Saldanha, M. Studies on the mechanisms of lead immobilization by hydroxyapatite. *Environ. Sci. Technol.* **2002**, *36*, 1625−1629.
(33) Jeanjean, J.; Vincent, U.; Fedoroff, M. Structural modification of calcium hydroxyapatite induced by sorption of cadmium ions. *J. Solid State Chem.* **1994**, *108*, 68−72.
(34) Leyva, A. G.; Marrero, J.; Smichowski, P.; Cicerone, D. Sorption of antimony onto hydroxyapatite. *Environ. Sci. Technol.* **2001**, *35*, 3669−3675.
(35) Vega, E. D.; Pedregosa, J. C.; Narda, G. E.; Morando, P. J. Removal of oxovanadium (IV) from aqueous solutions by using commercial crystalline calcium hydroxyapatite. *Water Res.* **2003**, *37*, 1776−1782.
(36) Ma, Q. Y.; Logan, T. J.; Traina, S. J.; Ryan, J. A. Effects of aqueous Al, Cd, Cu, Fe (II), Ni, and Zn on Pb immobilization by hydroxyapatite. *Environ. Sci. Technol.* **1994**, *28*, 1219−1228.

DOI: 10.1021/ie504181z
Ind. Eng. Chem. Res. 2015, 54, 585−596

(37) Daniels, Y.; Alexandratos, S. D. Design and synthesis of hydroxyapatite with organic modifiers for environmental remediation. *Waste Biomass Valor.* **2010**, *1*, 157−162.
(38) Jang, S. H.; Jeong, Y. G.; Min, B. G.; Lyoo, W. S.; Lee, S. C. Preparation and lead ion removal property of hydroxyapatite/polyacrylamide composite hydrogels. *J. Hazard. Mater.* **2008**, *159*, 294−299.
(39) Jang, S. H.; Min, B. G.; Jeong, Y. G.; Lyoo, W. S.; Lee, S. C. Removal of lead ions in aqueous solution by hydroxyapatite/polyurethane composite foams, *J. Hazard. Mater.* **2008**, *152*, 1285−1292.
(40) Verwilghen, C.; Rio, S.; Nzihou, A.; Gauthier, D.; Flamant, G.; Sharrock, P. J. Preparation of high specific surface area hydroxyapatite for environmental applications. *J. Mater. Sci.* **2007**, *42*, 6062−6066.
(41) Nancollas, G. H.; Tang, R.; Phipps, R. J.; Henneman, Z.; Gulde, S.; Wu, W.; Mangood, A.; Russell, R. G. G.; Ebetino, F. H. Novel insights into actions of bisphosphonates on bone: Differences in interactions with hydroxyapatite. *Bone* **2006**, *38*, 617−627.
(42) Henneman, Z. J.; Nancollas, G. H.; Ebetino, F. H.; Russell, R. G.; Phipps, R. G. Bisphosphonate binding affinity as assessed by inhibition of carbonated apatite dissolution in vitro. *J. Biomed. Mater. Res. Part A* **2008**, *85A*, 993−1000.
(43) Lawson, M. A.; Xia, Z.; Barnett, B. L.; Triffitt, J. T.; Phipps, R. J.; Dunford, J. E.; Locklin, R. M.; Ebetino, F. H.; Russell, R. G. Differences between bisphosphonates in binding affinities for hydroxyapatite. *J. Biomed. Mater. Res. Part B* **2009**, *92B*, 149−155.
(44) Deluchat, V.; Bollinger, J.; Serpaud, B.; Caullet, C. Divalent cations speciation with three phosphonate ligands in the pH-range of natural waters. *Talanta* **1997**, *44*, 897−907.
(45) Popov, K.; Ronkkomami, H.; Lajunen, L. H. Critical evaluation of stability constants of phosphonic acids. *J. Pure Appl. Chem.* **2001**, *73* (10), 1641−1677.
(46) Saeri, M. R.; Afshar, A.; Ghorbani, M.; Ehsani, N.; Sorrell, C. C. The wet precipitation process of hydroxyapatite. *Mater. Lett.* **2003**, *57*, 4064−4069.
(47) Daniels, Y.; Zhu, X.; Alexandratos, S. D. Distinguishing between organic and inorganic phosphorus in hydroxyapatite by elemental analysis. *Microchem. J.* **2013**, *110*, 263−265.
(48) Ober, R. D. Synthesis and Development of Selective Ion-Exchange Resins for the Removal of Toxic Metal Ions from Water in the Environment, Ph.D. Dissertation, University of Tennessee at Knoxville, 1999.
(49) Dong, L.; Zhu, Z.; Qiu, Y.; Zhao, J. Removal of lead from aqueous solution by hydroxyapatite /magnetite composite adsorbent. *Chem. Eng. J.* **2010**, *165*, 827−834.
(50) Bengtsson, A.; Shchukarev, A.; Persson, P.; Sjoberg, S. A solubility and surface complexation study of a non-stoichiometric hydroxyapatite. *Geochim. Cosmochim. Acta* **2009**, *73*, 257−267.
(51) Miquel, J. L.; Facchini, L.; Legrand, A. P.; Rey, C. Lemaitre, Solid-state NMR to study calcium-phosphate ceramics. *J. Colloids Surf.* **1990**, *45*, 427−433.
(52) Carman, R.; Edlund, G.; Damberg, C. Distribution of organic and inorganic phosphorus compounds in marine and lacustrine sediments: A P-31 NMR study. *Chem. Geol.* **2000**, *163*, 101−114.
(53) Bouazza, D.; Miloudi, H.; Sassi, M.; Boos, A.; Goetz, G.; Tayeb, A.; Bengueddach, A. Preparation of montmorillonite clays containing DTMPPA for zinc extraction. *J. Phys. Chem. Solids* **2006**, *67*, 1032−1036.
(54) Browning, F. H.; Fogler, H. S. Effect of precipitating conditions on the formation of calcium−HEDP precipitates. *Langmuir* **1996**, *12*, 5231−5238.
(55) Belkhouche, N.-E.; Didi, M. A.; Romero, R.; Jonsson, J. A.; Villemin, D. Study of new organophosphorus derivates carriers on the selective recovery of M (II) and M (III) metals, using supported liquid membrane extraction. *J. Membr. Sci.* **2006**, *284*, 398−405.
(56) Misono, M.; Ochiai, E.; Saito, Y.; Yoneda, Y. New dual parameter scale for the strength of Lewis acids and bases with the evaluation of their softness. *J. Inorg. Nucl. Chem.* **1967**, *29*, 2685−2691.
(57) Alexandratos, S. D.; Zhu, X. Bifunctional coordinating polymers: auxiliary groups as a means of tuning the ionic affinity of immobilized phosphate ligands. *Macromolecules* **2005**, *38*, 5981−5986.

DOI: 10.1021/ie504181z
Ind. Eng. Chem. Res. 2015, 54, 585−596